International Journal of Applied Earth Observation and Geoinformation 13 (2011) 586–594

Contents lists available at ScienceDirect

International Journal of Applied Earth Observation and Geoinformation

journal homepage: www.elsevier.com/locate/jag

Quantitative urban climate mapping based on a geographical database: A simulation approach using Hong Kong as a case study

Liang Chen*, Edward Ng

School of Architecture, The Chinese University of Hong Kong, Shatin, N.T., Hong Kong, China

ARTICLE INFO

Article history:
Received 11 October 2010
Accepted 15 March 2011

Keywords:
Urban climate mapping
Geographical information system
Urban simulation
Sky view factor
Frontal area density

ABSTRACT

The urban environment has been dramatically changed by artificial constructions. How the modified urban geometry affects the urban climate and therefore human thermal comfort has become a primary concern for urban planners. The present study takes a simulation approach to analyze the influence of urban geometry on the urban climate and maps this climatic understanding from a quantitative perspective. A geographical building database is used to characterize two widely discussed aspects: urban heat island effect (UHI) and wind dynamics. The parameters of the sky view factor (SVF) and the frontal area density (FAD) are simulated using ArcGIS-embedded computer programs to link urban geometry with the UHI and wind dynamic conditions. The simulated results are synergized and classified to evaluate different urban climatic conditions based on thermal comfort consideration. A climatic map is then generated implementing the classification. The climatic map shows reasonable agreement with thermal comfort understanding, as indicated by the biometeorological index of the physiological equivalent temperature (PET) obtained in an earlier study. The proposed climate mapping approach can provide both quantitative and visual evaluation of the urban environment for urban planners with climatic concerns. The map could be used as a decision support tool in planning and policy-making processes. An urban area in Hong Kong is used as a case study.

1. Introduction

Urbanization is inevitable. More than half of the world's population currently lives in cities (Population Reference Bureau, 2009), and this number is anticipated to reach 60% (or 4.9 billion) by the year 2030 (UNFPA, 2007). A direct consequence of this rapid and continuing urbanization process is that the environment has been severely changed by artificial development and construction. Natural vegetation has been removed and natural terrain has been altered and mounted densely with high-rise buildings. The result is a new type of geometry (i.e., the urban geometry) that has significant impacts on the microclimate in the urban environment. Differences in surface material and geometric form result in the widely observed and discussed urban heat island effect (UHI) (Arnfield, 2003), and building bulks dramatically modify the aerodynamic environment in cities (Oke, 1987). Consequently, human thermal comfort and urban living quality are greatly affected.

Climatic issues have been increasingly recognized in building design and urban planning (Oke, 1988; Givoni, 1998; Eliasson, 2000; Cleugh et al., 2009). Urban planners and decision makers, faced with the task of designing urban environments that promote high living quality, are always in great need of knowledge transfer and decision support tools. Hong Kong (22°15′N, 114°10′E) is one of the world's densest cities, with its more than 7 million inhabitants living in approximately 260 km^2 of land. With its hot and humid subtropical climate, it is faced with challenges in urban development that are not experienced by any other metropolises around the world. Under these circumstances, urban climatic considerations have been increasingly recognized in the development of planning standards and guidelines. A series of governmental and research projects have been conducted to study the impact of the urban environment on outdoor thermal comfort, with the objective of providing implications for planning and design (Planning Department, 2005, 2008; Ng, 2009).

The objective of the present study is to translate climatic understanding into analytical maps that provide quantitative information for decision making. Two main climatic impacts are considered: UHI and wind dynamics. A simulation approach using a geodatabase to characterize the urban geometry is conducted. A densely built-up area in Hong Kong, the Kowloon peninsula, is used as a case study. The study site is a 4 km × 5.6 km coastal area with

* Corresponding author at: Room 701, Wong Foo Yuan Building, School of Architecture, The Chinese University of Hong Kong, Shatin, N.T., Hong Kong, China. Tel.: +852 26096597.
E-mail addresses: chenliang@cuhk.edu.hk, chenliangcl@gmail.com (L. Chen).

0303-2434/$ – see front matter © 2011 Elsevier B.V. All rights reserved.
doi:10.1016/j.jag.2011.03.003

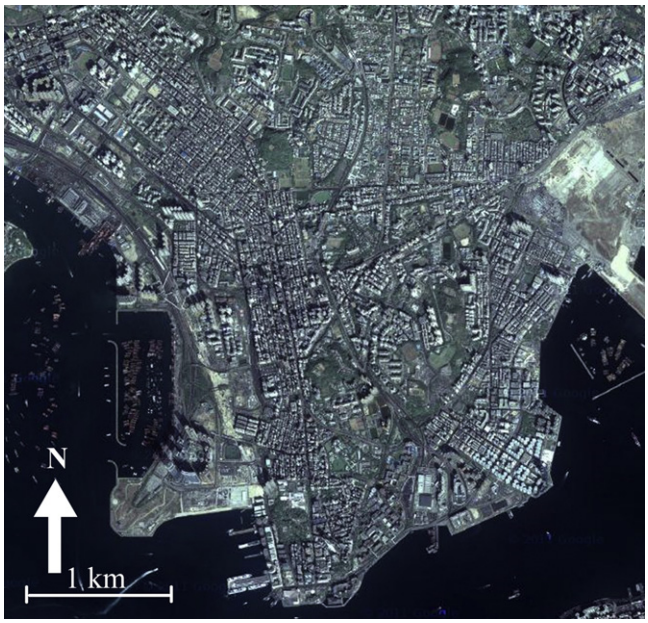

Fig. 1. Google™ map of the study site: the Kowloon peninsula.

flat terrain and little vegetation, as shown in Fig. 1. Building form is therefore the dominant factor in affecting the local urban climate.

2. Background

2.1. Urban climatic map

Mapping urban climatic information for planning purposes is not a novel idea. Its basic landscape was developed in the 1990s in the institutional guidelines of Germany (VDI, 1997). In the last decade, climatic mapping has been applied to a number of governmental and research projects across the world, including the Urban Climate 21 program in Stuttgart, Germany (Office for Environmental Protection, N/A); the Climatological Air Temperature Map in Poland (Ustrnul and Czekierda, 2005); the Urban Environmental Climate Map in Japan (Tanaka et al., 2009); the Bioclimatic Map in Portugal (Alcoforado et al., 2009); the Local Climate Zone Map in Canada (Stewart and Oke, 2009), and the Urban Climatic Map in Hong Kong (Planning Department, 2008). Despite their different specialties and implementation methods, these projects all aim to provide visual and also analytical information for planners. Svensson et al. (2003) have introduced a GIS-based approach to implement urban climatic mapping systems. The practical GIS application makes the climatic information useful for urban planning easily accessible to planners.

Among many examples, the Hong Kong Climatic Map takes a bioclimatic approach by classifying the urban territory into different classes, corresponding to different human thermal comfort conditions, as described by the biometeorological index of the physiological equivalent temperature (PET) (Mayer and Höppe, 1987). Climatic factors considered include building density, topography, ground roughness and greenery. Thermal load and wind dynamics are used as bases for evaluating the urban microclimatic condition (Ng, in press). Because the project is an initial investigation along this line of research, the modeling and classification of the urban microclimate are mainly based on preliminary findings obtained in empirical studies and uses simple parameters such as building volume and site coverage. Other studies have suggested the usefulness of morphometric indicators, such as the sky view factor and the roughness length of building form, in describing the thermal and aerodynamic characteristics of urban environment (Oke, 1987; Grimmond and Oke, 1999). However, these indicators cannot be easily derived from the aforementioned parameters. Under such circumstances, a systematic and quantitative methodology to facilitate the development of urban climate mapping systems of this kind with more effective descriptions of the urban form is needed.

2.2. The simulation approach in urban climatology

The simulation approach has been increasingly adapted in urban climatology studies (Arnfield, 1990; Ratti et al., 2002; Gal and Sumeghy, 2007; Lindberg, 2007; Gal and Unger, 2008; Unger, 2009). In contrast to conventional remote-sensing methods (Nichol, 2005; Hung et al., 2006), the simulation approach reconstructs the physical urban environment in a silicon surrogate, and characterizes the spatial variation of quantities and relationships of the urban environment. Its integration with GIS platforms is particularly suitable for spatially related investigations. Geo-databases are normally used, including vector or raster data (Gal et al., 2009). In particular, the digital elevation model (DEM) is a raster format containing 3-D information on 2-D digital support. It is considered "not as a simple store of information, but as a tool for supporting many forms of analysis." (Falcidieno, 1994) Indeed, because of its direct connection with GIS systems, DEM has found its most common applications in geographical studies (Lin and Oguchi, 2006; Ruiz-Arias et al., 2009; Tarekegn et al., 2010). However, although the usefulness of DEM in modeling urban geometry in climatology studies has been confirmed (Ratti and Richens, 2004; Lindberg, 2007), related analyses and applications in the urban context remain sparse. In the present study, a DEM database with building height information is used to model the urban morphology.

3. Simulation methodology

The present study employs two well-developed parameters to quantify the UHI and wind dynamic environment of Hong Kong's urban environment: the sky view factor (SVF) (Watson and Johnson, 1987) and the frontal area density (FAD) (Burian et al., 2002). Computer programs are developed for this purpose, and high-resolution DEM database in 2 m resolution is used as input, as shown in Fig. 2.

3.1. Sky view factor simulation

The sky view factor (SVF), commonly denoted by ψ_{sky}, indicates the ratio between the radiation received by a planar surface from the sky to the radiation emitted to the entire hemispheric radiating environment (Watson and Johnson, 1987). It is a dimensionless value ranging from 0 to 1, where $\psi_{sky} = 0$ means that the sky is completely obstructed and the outgoing long-wave radiation is trapped in the urban canyons, and $\psi_{sky} = 1$ means that the sky is completely open and the radiation is freely emitted outside the urban canopy layer. Because of its important role in energy balance schemes, SVF has been commonly adapted to relate the urban geometry with UHI in urban climatology studies (Unger, 2004). In short, lower SVF indicates stronger UHI, and vice versa.

In the present study, an ArcGIS-embedded computer program is developed for calculating SVF. The algorithm is introduced in (Chen et al., in press) and has been proven to provide accurate estimation of SVF compared with fish-eye lens photos. Fig. 3 shows an illustration of the algorithm. Briefly, the method divides the hemispheric radiating environment with radius R into equal slices by a rotation angle α, and searches for a building with the largest elevation angle β along a particular direction. The elevation angle is calculated by the building height, which is read from the DEM database. If such a building is found, then the surface, S, it obstructs is considered as

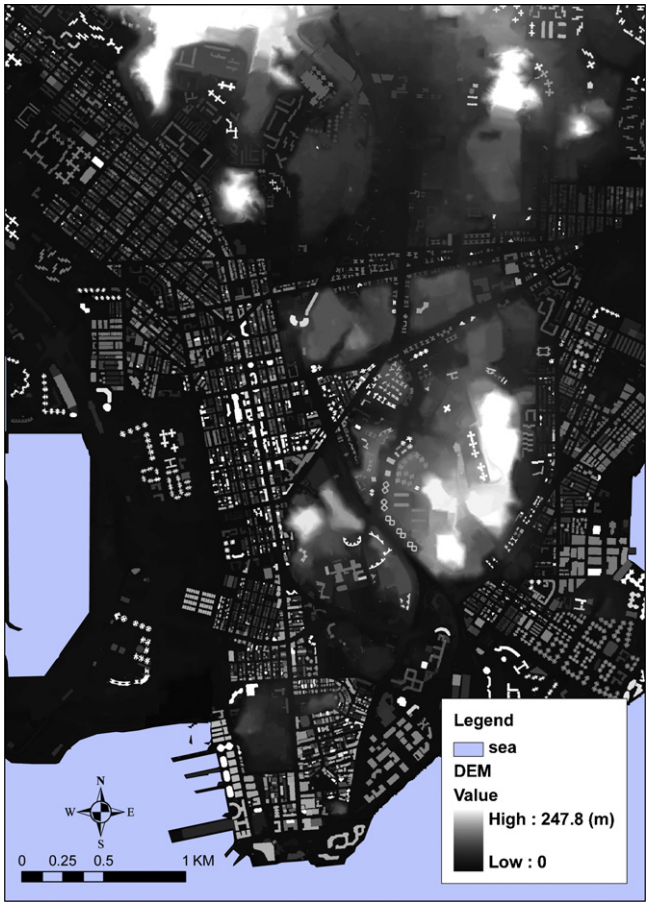

Fig. 2. A DEM (digital elevation model) map of the study site. The map is in 2 m resolution.

a slice of an enclosed basin, as examined by Oke (1987). The view factor of S is then calculated as follows:

$$VF(S) = (1 - \cos^2 \beta) \cdot \left(\frac{\alpha}{360}\right) = \sin^2 \beta \cdot \left(\frac{\alpha}{360}\right) \quad (1)$$

After obtaining the $VF(S)$ for all directions, SVF can be calculated by summing up all the $VF(S)$ and subtracting the sum from unity. The calculation is conducted entirely in the ArcGIS software, and

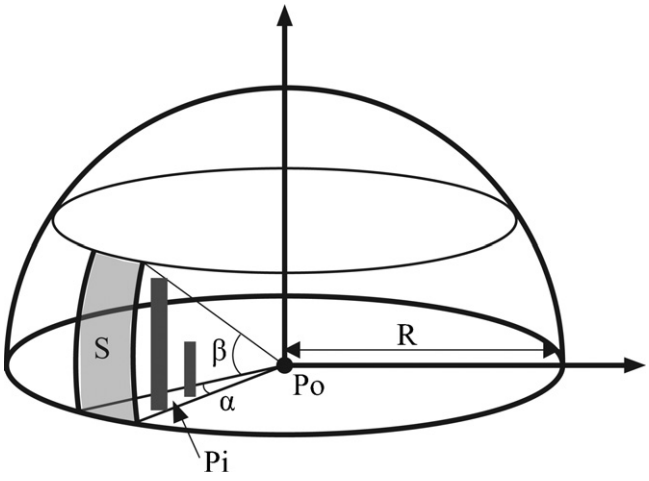

Fig. 3. Illustration of the algorithm for calculating SVF. *Po* is the pixel whose SVF is to be calculated. α is the rotation angle and R is the searching radius. *Pi* is the pixel with the largest elevation angle β along a certain direction. Surface S is the segment of the sky obstructed by *Pi*.

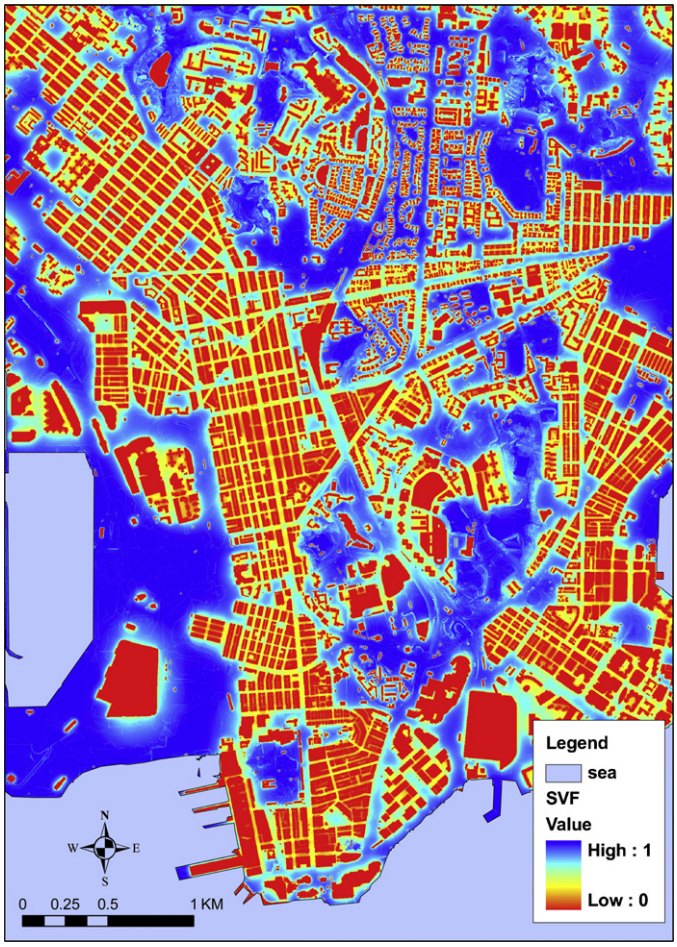

Fig. 4. Ground-level continuous SVF map for the study site. The map is in 2 m resolution.

the result is saved as a raster-format map. Fig. 4 shows the 2 m resolution ground-level SVF map of Kowloon. This map presents the spatial distribution of the thermal load due to differences in building mass: higher SVF value indicates lower thermal load, and lower SVF value indicates higher thermal load.

3.2. Frontal area density simulation

The frontal area density (FAD) is a measure of the frontal area per unit horizontal area per unit height increment. It has been widely used by researchers in the plant canopy and urban canopy communities to help quantify the drag force as a function of building height. The frontal area density $[a_f(z)]$ is defined as follows:

$$a_f(z, \theta) = \frac{A(\theta)_{proj(\Delta Z)}}{A_T \, \Delta z} \quad (2)$$

where $A(\theta)_{proj(\Delta Z)}$ is the area of building surfaces projected into the plane normal to the approaching wind direction for a specified height increment Δz; θ is the wind direction angle; and A_T is the total plan area of the study site. For a specified wind direction, the integral of $a_f(z)$ over the canopy height equals the roughness length λf (Burian et al., 2002).

In the present study, an ArcGIS-embedded computer program is developed to calculate FAD. The algorithm is modified after the methods proposed by (Grimmond and Oke, 1999; Burian et al., 2002), however it uses high-resolution DEM as input. Fig. 5 illustrates the spatial layout of the algorithm. For a particular wind direction, the algorithm calculates the "effective" building frontal

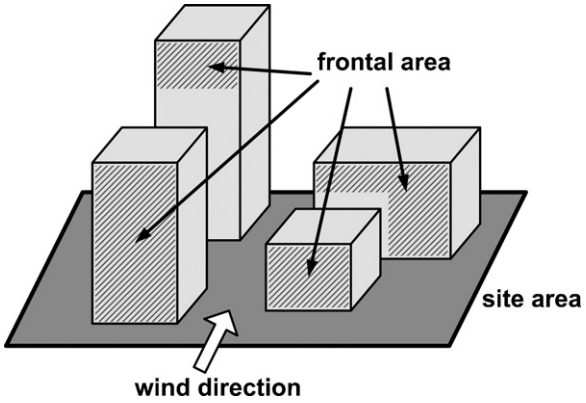

Fig. 5. Illustration of the spatial layout for the algorithm for calculating FAD for a site. The site area is selected to be 100 m × 100 m in practice.

area projected to the plane normal to the direction. Being "effective" means that the blocked area of a leeward building is not considered in the calculation, which is done by comparing the height difference between the windward and leeward buildings based on the DEM. A notable feature of the developed program is that it is able to account for complex wind environment in the real-world context. In practice, the MM5 (a numerical model for simulating atmospheric circulation) data obtained from the Hong Kong University of Science and Technology (Yim et al., 2007) are input as wind information. Wind roses with 16 wind directions are used, representing the wind environment of the study domain in the real world. The computer program reads the wind rose data and derives the total FAD for a site by calculating the weighted summation of the FAD for all wind directions. An earlier study in Hong Kong (Wong et al., 2010) uses a site area of 100 m × 100 m for the FAD calculation, which is also adapted in this study. Fig. 6 shows the resulting 100 m resolution FAD map of Kowloon. This map presents the spatial variation of the wind environment influenced by building bulks: higher FAD value indicates lower wind speed, whereas lower FAD value indicates fewer blockages of wind and, therefore, higher wind speed.

4. Climatic mapping methodology

This section introduces the methodology that integrates the UHI and wind dynamic characteristics of the urban environment, quantified by SVF and FAD, respectively, and assesses the climatic condition of the urban environment with concerns on human thermal comfort. A typical summer afternoon scenario is considered because it is the most crucial season for Hong Kong. The classified UHI and wind dynamic conditions are synergized and a climatic map is presented.

4.1. UHI mapping

In a previous study (Chen et al., in press), SVF has been shown as having a strong negative relationship with daytime intra-urban air temperature differences: a decrease of approximately 0.15 in the areal average of SVF results in 1 °C temperature elevation in street canyons. Based on this finding, a conservative estimation of the spatial variation of intra-urban temperature is given as: SVF smaller than 0.35 indicates 3 °C temperature elevation, SVF within [0.35, 0.50] indicates 2 °C temperature elevation, SVF within [0.50, 0.65] indicates 1 °C temperature elevation, and SVF larger than 0.65 indicates no temperature elevation within the urban area. The SVF map generated in Section 3.1 is aggregated to 100 m resolution and classified based on this relationship in order to link with air temperature variations. The resulting thermal load class map is shown in Fig. 7. In the map, a class value difference of 1 indicates 1 °C temperature difference.

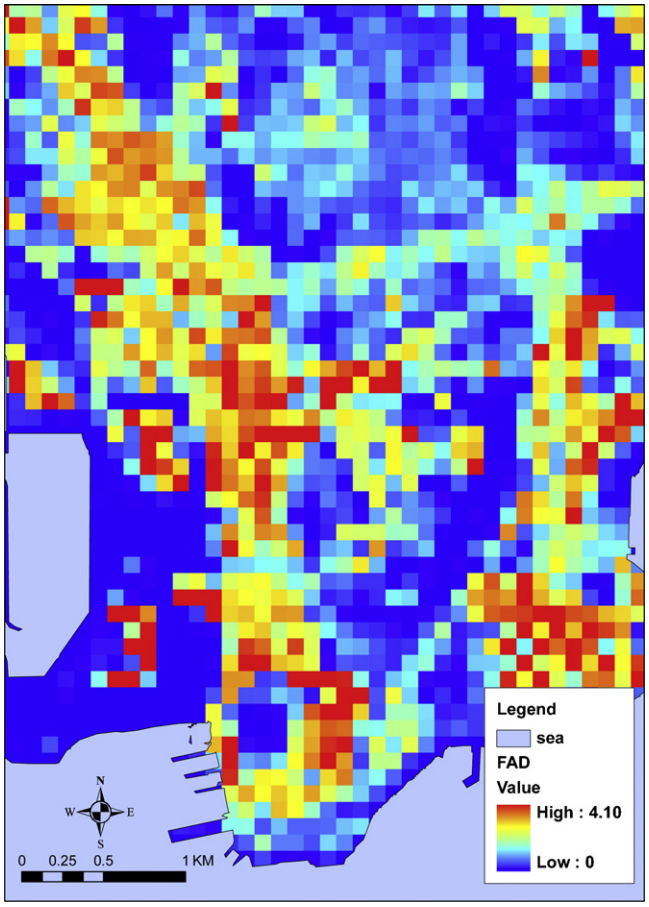

Fig. 6. FAD map for the study site. The map is in 100 m resolution.

4.2. Wind dynamic mapping

According to Oke (1987), the roughness length of urban structure has a direct relationship with the wind velocity: the larger the roughness length, the lower the wind velocity, following a logarithmic relationship. An earlier study shows that, in the Hong Kong urban area, a 0.7 m/s increase in wind velocity is equivalent to 1.9 °C air temperature mitigation in thermal comfort terms in summer (Cheng et al., in press). This relationship is approximated by equaling 0.4 m/s wind velocity increase to 1 °C temperature mitigation in thermal comfort terms. Based on these findings, the FAD map is classified such that FAD smaller than 0.25 indicates 2 °C temperature mitigation, FAD within [0.25, 0.8] indicates 1 °C temperature mitigation, and FAD larger than 0.8 indicates no temperature mitigation. The resulting wind dynamic class map is shown in Fig. 8. The class values are negative, indicating the mitigation effect.

As a tentative approach, the two maps are combined by linear summation using simple map algebra to evaluate the overall impact of building form on temperature variations. The generated climatic map is shown in Fig. 9. The resulting climatic map shows a diverse pattern of the study site, with six climatic classes ranging from −2 to +3. Positive value indicates thermal discomfort (high heat stress and weak ventilation), whereas negative value indicates the opposite (i.e., the mitigation effect that promotes thermal comfort). A zero value indicates the "neutral" condition, pertaining to human's neutral thermal comfort sensation from moderate heat stress and brisk wind.

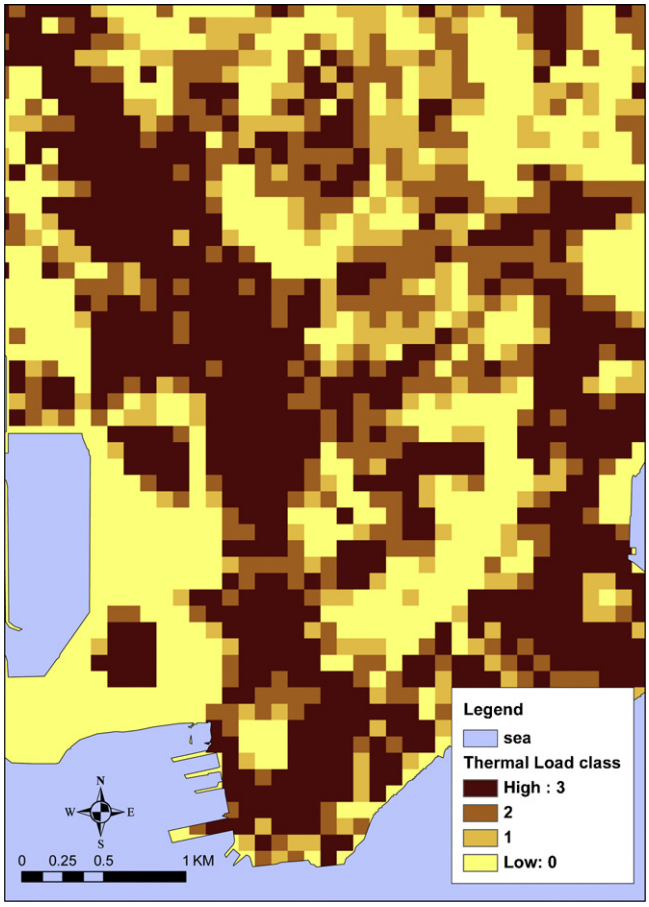

Fig. 7. Thermal load map for the study site derived from SVF classification. Higher value indicates higher thermal stress due to building mass, and vice versa. The map is in 100 m resolution.

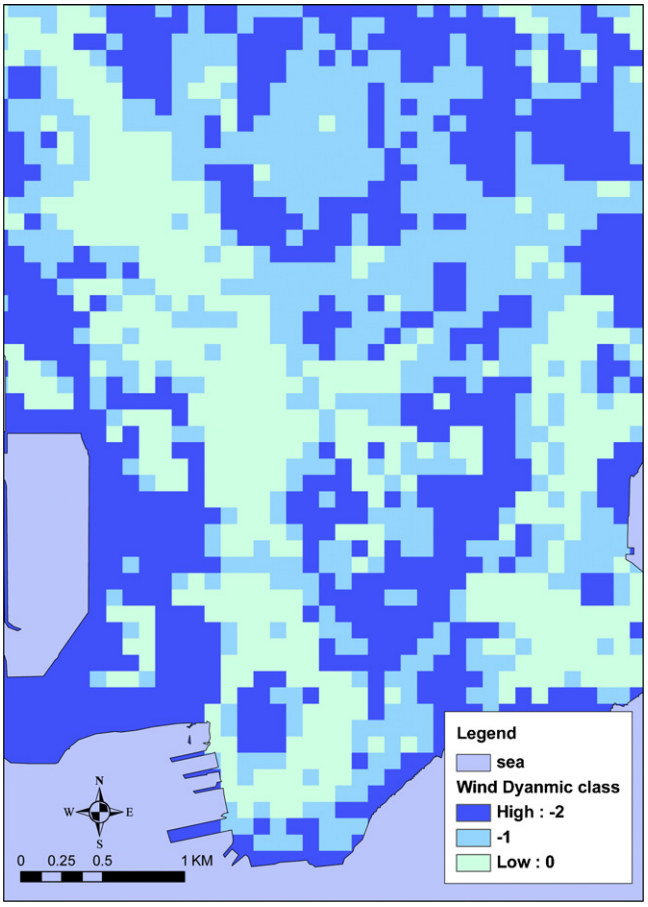

Fig. 8. Wind dynamic map for the study site derived from FAD classification. Higher value indicates higher wind dynamic (i.e., higher wind speed). The map is in 100 m resolution.

5. Analysis and discussion

5.1. Comparison between the climatic map classes and PET

To quantitatively test the validity of the climatic map, it is compared with the biometeorological thermal comfort index of PET calculated based on meteorological data obtained from on-site spot measurements. The measurements were carried out in summer afternoons from early September to October in 2008. Detailed specifications of the measurements are given in Ng et al. (2008c). Fig. 10 shows the mobile meteorological station used in the measurements. Variables measured include air temperature, solar radiation, wind velocity and relative humidity. Air temperature (T_a), wind velocity (V), and relative humidity were measured using the TESTO three-function sensor probes. Solar radiation was measured as the globe temperature (T_g) using a tailor-made globe thermometer. The datalogger was set at a sampling rate of 10 s and an averaging time of 10 min. The mean radiant temperature (T_{mrt}) was calculated using the equation proposed by ASHRAE (2001):

$$T_{mrt} = \left[(T_g + 273)^4 + \frac{1.10 \times 10^8 V^{0.6}}{\varepsilon D^{0.4}} (T_g - T_a) \right]^{1/4} - 273 \qquad (3)$$

where ε is emissivity and $\varepsilon = 0.95$ for the black globe thermometer; D is the globe diameter and $D = 0.038$m; V is wind velocity in m/s; T_a is air temperature in °C; and T_g is globe temperature in °C.

The average data from three measurements covering 10 points in the site are used. The PET value for each point is calculated, indicating the thermal comfort level of a standard person (male, 1.75 m tall, 75 kg, and 35 years old). The PET value points are digitized into the climatic map using the ArcGIS software. The climatic map class value for each point is extracted using ArcGIS built-in functions. The PET values are correlated with the local climatic classes using linear regression with a significance level of 5%. The regression result is shown in Fig. 11.

The regression result proves the validity of the climatic classes from three aspects: (1) the climatic classes correlate with the PET values reasonably well, with determination coefficient R^2 in the order of 0.698 (however, one single point shows substantial discrepancy, with the cause being currently unclear); (2) the correlation coefficient is 0.96, indicating that a climatic class value of 1 can closely correspond to 1 °C of PET; and (3) previous studies have shown that the neutral PET in Hong Kong's summer is approximately 29 °C (Ng et al., 2008a). Fig. 11 shows that the climatic class of 0, which is the neutral climatic condition, corresponds to approximately 28.5 °C in PET, which is in agreement with the early findings. The usefulness of the presented climatic mapping methodology is confirmed, suggesting that the map can provide substantial explanatory power in identifying the urban climatic conditions in Hong Kong's urban environment.

5.2. Comparison between the simulation results and rough estimations

The simulation approach considers the third dimension and calculates parameters such as SVF and FAD, which have been proven effective indicators in quantifying the impact of urban geometry on urban microclimate. This is compared with the preliminary attempt

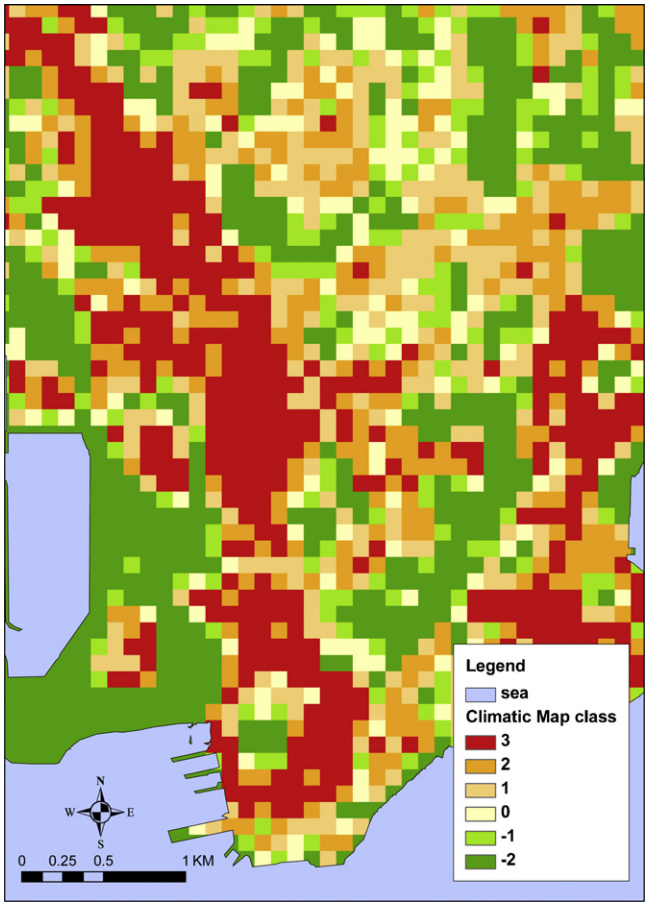

Fig. 9. Climatic map for the study site derived by adding the thermal load map and the wind dynamic map together. Positive value indicates thermal discomfort, while negative value indicates the opposite (i.e., the mitigation effect that promotes thermal comfort). A zero value indicates the "neutral" condition. The map is in 100 m resolution.

in the previously mentioned Hong Kong Urban Climatic Map Project (Ng et al., 2008b), which uses building volume and site coverage to estimate UHI and wind speed, respectively. This section conducts comparisons between the simulation results and the rough estimations.

5.2.1. Comparison between SVF and building volume

The relationship between SVF and building volume has been extensively discussed using various parametric models in (Chen et al., in press). They normally follow a logarithmic relationship for buildings with regular shapes and symmetrical layouts. SVF decreases as building volume increases, suggesting that building volume could be used as approximate estimation of SVF for simple regular conditions. However, the building shapes and layouts in reality are normally very complex, which brings into question the applicability of building volume; thus, a comparison test is necessary. The sample sites are shown in Fig. 12. In Zone 1, most of the buildings have similar rectangular shapes and are tightly packed, representing the regular case. Zone 2 represents the complex case with more buildings with irregular shapes and variant layouts. SVF maps for each zone are calculated. The results are aggregated to 100 m resolution and compared with 100 m resolution building volume maps through regression analysis. Notably, the building volume is first normalized using the maximum building volume value in the domain before the comparison. Figs. 13 and 14 show the regression results for the two cases. For the regular case, SVF and building volume have a fairly strong logarithmic relationship, with determination coefficient R^2 in the order of 0.633. For the complex case, the relationship is much weaker, with R^2 in the order of 0.383. These results prove that SVF is a more suitable indicator to describe building density in relating with temperature variation for complex urban environment in the real world.

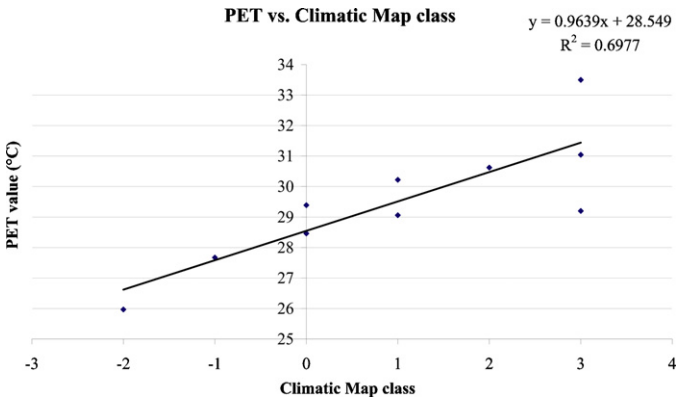

Fig. 11. Correlation of the calculated PET value based on meteorological data obtained in the spot measurement with the local Climatic Map class.

5.2.2. Comparison between FAD and site coverage/floor area ratio (FAR)

The FAD simulation considers both the third dimension (building height) and the complex wind environment (wind rose). It has advantages in describing the ventilation condition because of build-

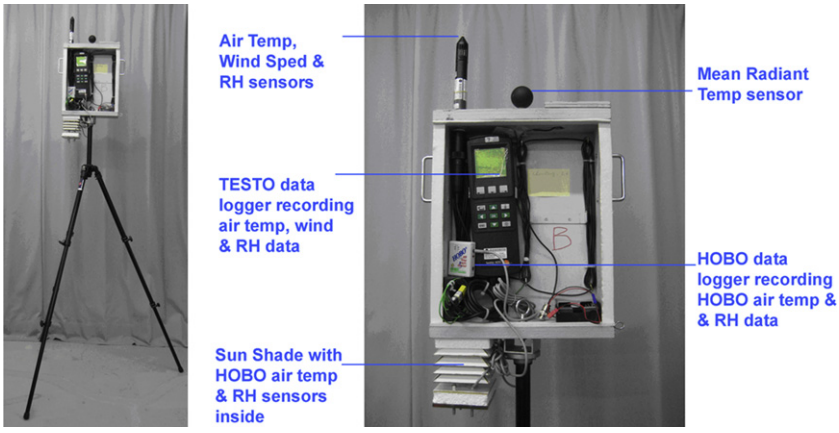

Fig. 10. Mobile meteorological station used in the on-site spot measurement.

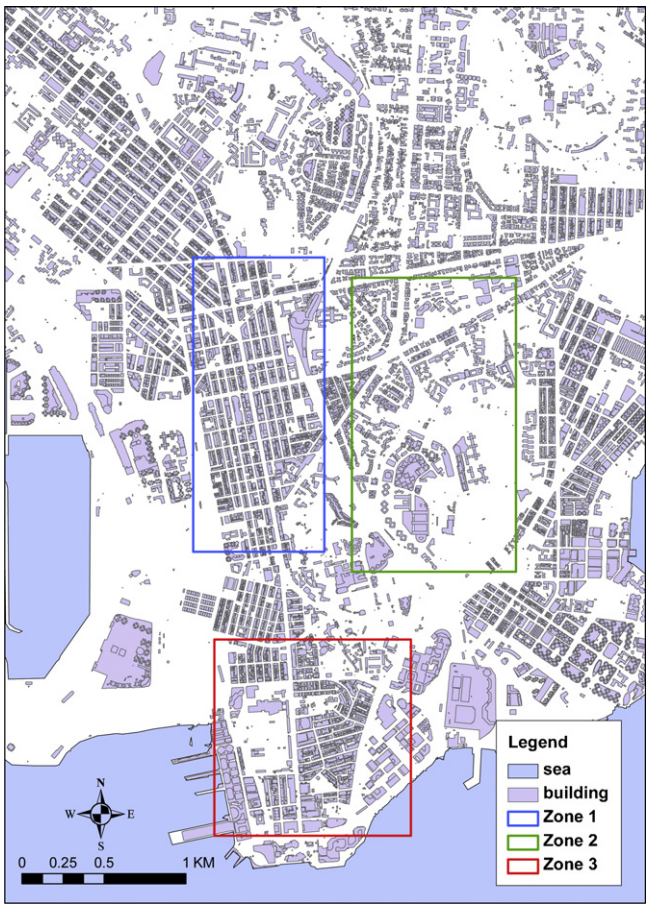

Fig. 12. Sample sites used in the comparison tests. Zone 1 and Zone 2 are used in the comparison between SVF and building volume. Zone 3 is used in the comparison between FAD and site coverage and FAR.

ing blockage in the real-world context compared to site coverage (i.e., the percentage of the area occupied by buildings) and floor area ratio (FAR) (i.e., the ratio of the total floor area to the site area). Thus, another comparison test is carried out using a sample area with various building heights and densities, as indicated by Zone 3 in Fig. 12. Site coverage and FAR for this area are calculated using 100 m × 100 m sites. The results are normalized with maximum values in domain, and compared with FAD using linear regression. Figs. 15 and 16 show the regression results. Notably, for the comparison between FAD and site coverage, only 20 randomly selected sites are shown to make the illustration sufficiently

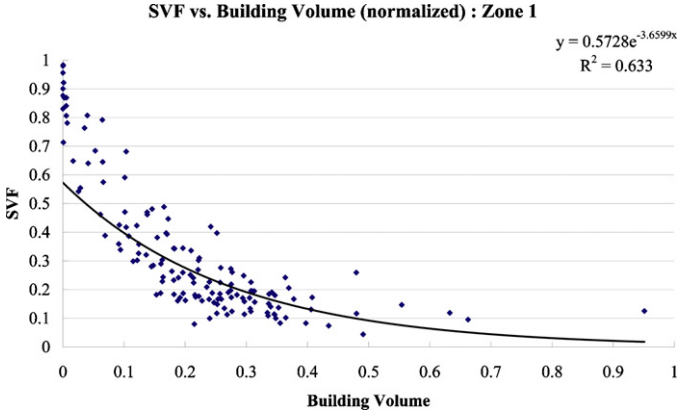

Fig. 13. Correlation of SVF and normalized building volume for Zone 1.

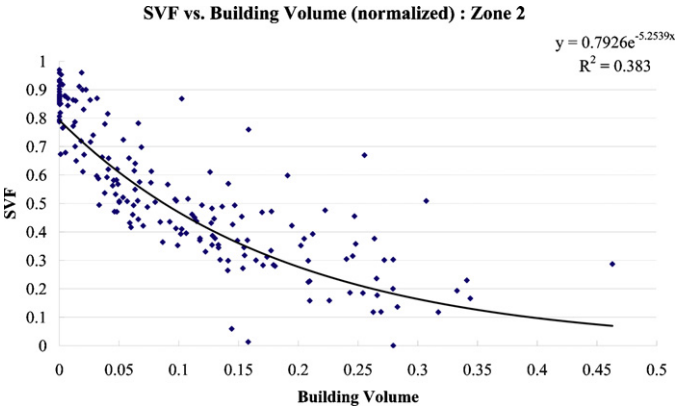

Fig. 14. Correlation of SVF and normalized building volume for Zone 2.

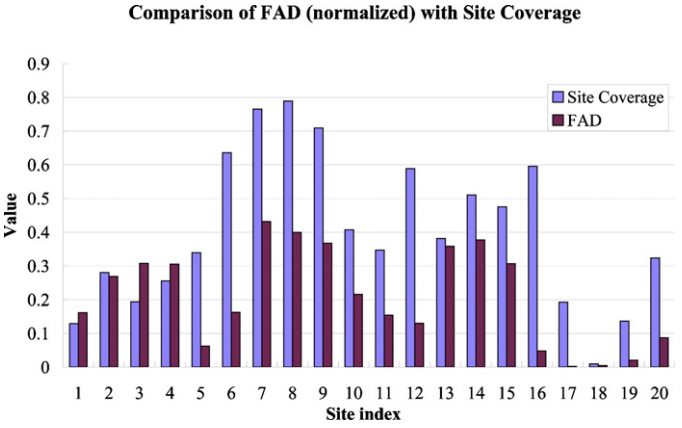

Fig. 15. Comparison of normalized FAD with site coverage for Zone 3.

detailed for observation purposes. Fig. 15 shows that, although higher site coverage generally indicates bigger FAD, significant discrepancies often occur (e.g., Sites 6 and 16 in the figure). This is as expected because site coverage does not concern building height, which plays an important role in determining FAD. In contrast, Fig. 16 shows that there is a proportional relationship between FAD and FAR, with R^2 in the order of 0.359. This suggests that FAR can be used as a rough estimation of the building roughness length. However, FAR does not discriminate between a big building and several smaller buildings with the same total floor area, and may therefore cause discrepancies in estimating FAD for high-density conditions, as illustrated by the relatively weak correlation in the figure.

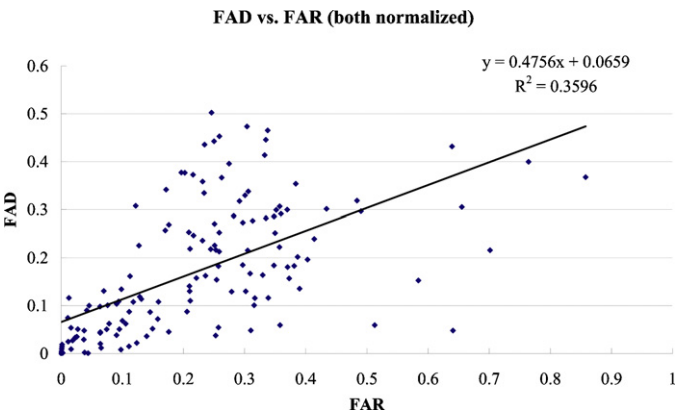

Fig. 16. Correlation of FAD with FAR (both are normalized).

The two comparison tests discussed above show that the estimations of building density and urban surface roughness can be improved by simulated SVF and FAD, respectively. Although the simulation requires greater computation resources, considering the high efficiency of the developed computer programs (less than 1 h for SVF simulation for the study site on a daily use PC, and approximately 10 s for FAD simulation), the usefulness of the simulation approach remains evident.

6. Conclusion

In the current study, a GIS-based simulation approach is presented to evaluate the microclimate of urban environment by means of SVF and FAD simulation. Computer programs embedded in the ArcGIS software are developed to calculate the SVF and FAD for an entire domain based on a DEM database. Classified SVF and FAD maps are used to account for the thermal load and wind dynamics of the urban environment, respectively, based on relationships found in empirical studies. A quantitative climatic map is generated, and validated with thermal comfort assessment using PET derived from on-site measurement. The good agreement suggests that the climatic map can be used as a decision support tool in urban planning and design with climatic concerns. Through comparison tests with rough estimation parameters, such as building volume and site coverage, the simulation approach has been proven to provide more effective descriptions of the urban geometry in relation with the urban microclimate. One limitation of the study is that it only considers the impact of building geometry on the urban microclimate. Other determinants, such as vegetation and topography, are expected to reveal more comprehensive understanding in future works.

Acknowledgements

The study is supported by a PGS grant from The Chinese University of Hong Kong and a contract research grant from the Planning Department, the Government of Hong Kong S.A.R. The authors wish to thank the Planning Department for providing the building data and also Prof. Jimmy Fung from Hong Kong University of Science and Technology for providing the MM5 access. Thanks also go to Mr. Max Lee and Miss. Chao Ren for preparing the measurement data.

References

Alcoforado, M.-J., Andrade, H., Lopes, A., Vasconcelos, J., 2009. Application of climatic guidelines to urban planning: the example of Lisbon (Portugal). Landscape and Urban Planning 90 (1–2), 56–65.

Arnfield, A.J., 2003. Review: Two decades of urban climate research: a review of turbulence, exchanges of energy and water, and the urban heat island. International Journal of Climatology 23, 1–26.

Arnfield, J., 1990. Canyon geometry, the urban fabric and nocturnal cooling: a simulation approach. Physical Geography 11, 220–239.

ASHRAE, 2001. ASHRAE Fundamentals Handbook 2001 (SI Edition). American Society of Heating, Refrigerating, and Air-Conditioning Engineers.

Burian, S.J., Brown, M.J., Linger, S.P., 2002. Morphological Analyses Using 3D Building Databases. Los Alamos National Laboratory, Los Angeles, CA, LA-UR-02-0781.

Chen, L., Ng, E., An, X., Ren, C., Lee, M., Wang, U., He, Z. Sky view factor analysis of street canyons and its implications for daytime intra-urban air temperature differentials in high-rise, high-density urban areas of Hong Kong: a GIS-based simulation approach. International Journal of Climatology, in press, doi:10.1002/joc.2145.

Cheng, V., Ng, E., Chan, C., Givoni, B. Outdoor thermal comfort study in sub-tropical climate: a longitudinal study based in Hong Kong. International Journal of Biometeorology, in press, doi:10.1007/s00484-010-0396-z.

Cleugh, H., Emmanuel, R., Endlicher, W., Erell, E., McGranahan, G., Mills, G., Ng, E., Nickson, A., Rosenthal, J., Steemer, K., 2009. Climate and sustainable cities: climate information for improved planning and management of mega cities (Needs and Capabilities Perspectives). In: Paper presented at World Climate Conference-3 (WCC-3) , Geneva, Swiztherland, 31 August–4 September.

Eliasson, I., 2000. The use of climate knowledge in urban planning. Landscape and Urban Planning 48, 31–44.

Falcidieno, B., 1994. Modelling and visualization of spatial data in GIS: Guest editor's introduction. Computers & Graphics 18 (6), 759–761.

Gal, T., Lindberg, F., Unger, J., 2009. Computing continuous sky view factors using 3D urban raster and vector databases: comparison and application to urban climate. Theoretical and Applied Climatology 95, 111–123.

Gal, T., Sumeghy, Z., 2007. Mapping the roughness parameters in a large urban area for urban climate applications. Acta Climatologica ET Chorologica 40–41, 27–36.

Gal, T., Unger, J., 2008. Detection of ventilation paths using high-resolution roughness parameter mapping in a large urban area. Building and Environment 44 (1), 198–206.

Givoni, B., 1998. Climate Considerations in Building and Urban Design. Van Nostrand Reinhold, New York.

Grimmond, C.S.B., Oke, T., 1999. Aerodynamic properties of urban areas derived from analysis of surface form. Journal of Applied Meteorology 38, 1261–1292.

Hung, T., Uchihama, D., Ochi, S., Yasuoka, Y., 2006. Assessment with satellite data of the urban heat island effects in Asian mega cities. International Journal of Applied Earth Observation and Geoinformation 8, 34–48.

Lin, Z., Oguchi, T., 2006. DEM analysis on longitudinal and transverse profiles of steep mountainous watersheds. Geomorphology 78 (1–2), 77–89.

Lindberg, F., 2007. Modelling the urban climate using a local governmental geodatabase. Meteorological Applications 14, 263–273.

Mayer, H., Höppe, P., 1987. Thermal comfort of man in different urban environments. Theoretical and Applied Climatology 38, 43–49.

Ng, E., 2009. Policies and technical guidelines for urban planning of high-density cities – air ventilation assessment (AVA) of Hong Kong. Building and Environment 44 (7), 1478–1488.

Ng, E. Towards planning and practical understanding of the need for meteorological and climatic information in the design of high-density cities: a case-based study of Hong Kong. International Journal of Climatology, in press, doi:10.1002/joc.2292.

Ng, E., Chan, C., Cheng, V., 2008a. Technical Input Report No. 1: Methodologies and Findings of User's Wind Comfort Level Survey. Urban Climatic Map and Standards for Wind Environment – Feasibility Study, Technical Report for Planning Department HKSAR. From http://www.pland.gov.hk/pland_en/p_study/prog_s/ucmapweb/ucmap_project/content/reports/Comfort_Level_Survey.pdf (last accessed: February 23, 2011).

Ng, E., Kwok, K., Sun, D., Yau, R., Katzschner, L., 2008b. Working Paper No. 1A: Draft Urban Climatic Analysis Map. Urban Climatic Map and Standards for Wind Environment – Feasibility Study, Technical Report for Planning Department HKSAR. From http://www.pland.gov.hk/pland_en/p_study/prog_s/ucmapweb/ucmap_project/content/reports/wp1a.pdf (last accessed: March 1, 2011).

Ng, E., Wang, U., Ren, C., Cheng, V., 2008c. Technical Input Report: Methodologies and Results of Field Measurement. Urban Climatic Map and Standards for Wind Environment – Feasibility Study, Technical Report for Planning Department HKSAR. From http://www.pland.gov.hk/pland_en/p_study/prog_s/ucmapweb/ucmap_project/content/reports/Field_Measurement.pdf (last accessed: February 23, 2011).

Nichol, J., 2005. Remote sensing of urban heat island by day and night. Photogrammetric Engineering and Remote Sensing 71 (5), 613–621.

Office for Environmental Protection, City of Stuttgart, N/A. Urban Climate Stuttgart 21. From http://www.stadtklima-stuttgart.de/index.php?climate_stuttgart_21_intro (last accessed: September 23, 2010).

Oke, T.R., 1987. Boundary Layer Climates, 2nd ed. Methuen, London.

Oke, T.R., 1988. Street design and urban canopy layer climate. Energy and Buildings 11 (1–3), 103–113.

Planning Department, the Government of Hong Kong S.A.R., 2005. Feasibility Study for Establishment of Air Ventilation Assessment System. From http://www.pland.gov.hk/pland_en/p_study/comp_s/avas/avas_eng.html (last accessed: February 5, 2011).

Planning Department, the Government of Hong Kong S.A.R., 2008. Urban Climatic Map and Standards for Wind Environment – Feasibility Study. From http://www.pland.gov.hk/pland_en/p_study/prog_s/ucmapweb/ucmap_project/content/content.html (last accessed: February 5, 2011).

Population Reference Bureau, 2009. 2009 World Population Data Sheet. From http://www.prb.org/Publications/Datasheets/2009/2009wpds.aspx (last accessed: September 23, 2010).

Ratti, C., Richens, P., 2004. Raster analysis of urban form. Environment and Planning B: Planning and Design 31, 297–309.

Ratti, C., Sabatino, S.D., Britter, R., Brown, M., Caton, F., Burian, S., 2002. Analysis of 3-D urban databases with respect to pollution dispersion for a number of European and American cities. Water, Air, & Soil Pollution: Focus 2, 459–469.

Ruiz-Arias, J.A., Tovar-Pescador, J., Pozo-Vaacutezquez, D., Alsamamra, H., 2009. A comparative analysis of DEM-based models to estimate the solar radiation in mountainous terrain. International Journal of Geographical Information Science 23 (8), 1049–1076.

Stewart, I., Oke, T., 2009. Newly developed "thermal climate zones" for defining and measuring urban heat island magnitude in the canopy layer. In: Paper presented at the 8th Symposium on the Urban Environment , Phoenix, AZ, 11–15 January.

Svensson, M.K., Thorsson, S., Lindqvist, S., 2003. A geographical information system model for creating bioclimatic maps – examples from a high, mid-latitude city. International Journal of Biometeorology 47 (2), 102–112.

Tanaka, T., Ogasawara, T., Koshi, H., Yoshida, S., Sadohara, S., Moriyama, M., 2009. Urban environmental climate maps for supporting urban-planning related work

of local governments in Japan: case studies of Yokohama and Sakai. In: Paper presented at the 7th International Conference on Urban Climate (ICUC-7), Yokohama, Japan, 29 June–3 July.
Tarekegn, T.H., Haile, A.T., Rientjes, T., Reggiani, P., Alkema, D., 2010. Assessment of an ASTER-generated DEM for 2D hydrodynamic flood modeling. International Journal of Applied Earth Observation and Geoinformation 12 (6), 457–465.
UNFPA, 2007. State of World Population 2007 – Unleashing the Potential of Urban Growth. United Nations Population Fund (UNPFA), New York.
Unger, J., 2004. Intra-urban relationship between surface geometry and urban heat island: review and new approach. Climate Research 27, 253–264.
Unger, J., 2009. Connection between urban heat island and sky view factor approximated by a software tool on a 3D urban database. International Journal of Environment and Pollution 36 (1/2/3), 59–80.
Ustrnul, Z., Czekierda, D., 2005. Application of GIS for the development of climatological air temperature maps: an example from Poland. Meteorological Applications 12, 43–50.
VDI, 1997. VDI Guideline 3787, Part 1: Environmental Meteorology – Climate and Air Pollution Maps for Cities and Regions. The Association of German Engineers.
Watson, I.D., Johnson, G.T., 1987. Graphical estimation of sky view-factors in urban environments. International Journal of Climatology 7 (2), 193–197.
Wong, M.S., Nichol, J.E., To, P.H., Wang, J., 2010. A simple method for designation of urban ventilation corridors and its application to urban heat island analysis. Building and Environment 45, 1880–1889.
Yim, S.H.L., Fung, J.C.H., Lau, A.K.H., Kot, S.C., 2007. Developing a high-resolution wind map for a complex terrain with a coupled MM5/CALMET system. Journal of Geophysical Research 112, D05106.